Dendrochronologia 96 (2026) 126507

Contents lists available at ScienceDirect

Dendrochronologia

journal homepage: www.elsevier.com/locate/dendro

Eastern white pine ring proxies show potential for climate reconstruction in a Canadian temperate forest

Julie-Pascale Labrecque-Foy [a,b,*], Marc-André Lemay [a,b], Fabio Gennaretti [a,b,c], Étienne Boucher [d], Dominique Arseneault [b,e], Miguel Montoro Girona [a,b,f]

[a] Groupe de recherche en écologie de la MRC Abitibi, Forest Research Institute, Université du Québec en Abitibi-Témiscamingue, Amos, Québec, Canada
[b] Center for Forest Research, Université du Québec à Montréal, Montréal, Québec, Canada
[c] Department of Agricultural, Food and Environmental Sciences, Università Politécnica delle Marche, Ancona, Italy
[d] Department of Geography, GEOTOP and Centre d'études nordiques, Université du Québec à Montréal, Montréal, Canada
[e] Université du Québec à Rimouski, Rimouski, Québec, Canada
[f] Grupo de Análisis y Planificación del Medio Natural, Universidad de Huelva, Huelva, Spain

A R T I C L E I N F O

Keywords:
Bayesian modeling
Climate change
Dendroclimatology
Pinus strobus
Stable isotopes
Tree rings

A B S T R A C T

High-resolution climate reconstructions are needed to understand past and future climate–vegetation dynamics. However, climate reconstructions using ring width are scarce in temperate regions where climate has limited impacts on tree growth. In Témiscamingue, white pine sunken logs represent valuable archives for long-term climate reconstructions, but white pine's response to climate variations in this temperate region is unknown. Moreover, the most suitable proxies for climate reconstruction in white pine—ring widths or stable isotopes—remain unclear. This study evaluates which proxy, or combination of proxies, best captures climate signals in white pine radial growth across contrasting soil drainage conditions. Ring widths were measured in 60 trees from Opémican National Park (30 on each of fast and moderate drainage conditions). Carbon and oxygen isotope ratios were analyzed from five trees per site over the period 1950–2020. Climatic data from ERA5 were used to calibrate response functions. June-August drought index (SPEI) as well as June-July precipitation and temperature were the dominant climatic drivers on all proxies, regardless of drainage type. Bayesian linear models revealed that combining carbon isotopes with ring-width data provided the most robust reconstruction of June–July precipitation ($r = 0.43$), that combining oxygen isotopes with ring widths yielded the best reconstruction of June–July temperatures ($r = 0.49$), and that combining carbon and oxygen isotopes produced the best reconstruction of June-August SPEI ($r = 0.45$). This study is among the first to demonstrate the potential of a multi-proxy approach for climate reconstruction using white pine. Our results provide insights that may guide future climate reconstructions in temperate regions, where tree species with lower climate sensitivity could also be considered.

1. Introduction

High-resolution climate reconstructions are key to understanding past and future climate–vegetation dynamics (Büntgen and Esper, 2025). Tree rings are widely used to reconstruct climatic conditions with annual resolution, and combining living and dead trees allows these reconstructions to be extended further back in time (Gennaretti et al., 2014; Grudd, 2008; Liu et al., 2017). Ring width generally reflects climate variations because tree growth is influenced, and sometimes limited, by environmental conditions (Duffy et al., 2019). However, in temperate regions where climate is less limiting and growth is influenced by multiple factors, it is more complex to study climate using tree-ring width (Shestakova and Martínez-Sancho, 2021). Some studies found that tree-ring isotopic composition can be more sensitive to climate variations in temperate regions, because they represent early response at the physiological level (Rinne et al., 2013; Sarris et al., 2013). This suggests that their use could be more appropriate for climate reconstruction in these regions. Moreover, many studies demonstrated that a multi-proxy approach combining ring width and isotopes (carbon [$\delta^{13}C$] and oxygen [$\delta^{18}O$]) could enhance common climatic signal and

* Corresponding author at: Groupe de recherche en écologie de la MRC Abitibi, Forest Research Institute, Université du Québec en Abitibi-Témiscamingue, Amos, Québec, Canada.
E-mail address: julie-pascale.labrecque-foy@uqat.ca (J.-P. Labrecque-Foy).

https://doi.org/10.1016/j.dendro.2026.126507
Received 10 September 2025; Received in revised form 26 January 2026; Accepted 14 March 2026
Available online 16 March 2026

reduce the error associated with individual proxies (Gennaretti et al., 2017; Hilasvuori et al., 2009; Sidorova et al., 2012).

To date, only one study has used white pine tree rings for climate reconstruction, focusing on winter climate in the Great Lakes region (Voelker et al., 2019). Nonetheless, because white pines are isohydric, they tend to respond rapidly to changes in temperature and precipitation (Asbjornsen et al., 2021), which makes them great candidates for summer climate reconstructions in temperate regions. Indeed, many studies have demonstrated their response to climate variations using tree-ring width (RW) and $\delta^{13}C$ isotopes (Asbjornsen et al., 2021; Chhin et al., 2018; Maier and Teskey, 1992). Before using white pine tree rings for climate reconstruction, it is necessary to assess the climate-tree ring relationship with living white pines over a period of time for which instrumental temperature and precipitations records are available (Gennaretti et al., 2017; Naulier et al., 2015). Moreover, the impact of different drainage levels on climatic signal of white pine should also be tested, because it is likely to modulate the response to climate and may introduce unwanted noise in climate reconstructions (Chhin et al., 2013).

Témiscamingue is a temperate region of eastern Canada where intensive harvesting of white pine (*Pinus strobus*) took place in the 19th and 20th centuries (Danneyrolles et al., 2016; Robles et al., 2025). The extensive exploitation of white pine forests is thought to have contributed to their declining abundance in Témiscamingue, leading to a recent need for restoration (Uprety et al., 2013). Early forest exploitation in Témiscamingue was accompanied by log driving – the floating of logs on waterways for their transportation (Aird, 2016; Sedell et al., 1991). White pine logs that sank during log driving are still well preserved and represent a valuable archive for reconstructing climate from the preindustrial period (before 1800) to the mid-20th century (Labrecque-Foy and Montoro Girona, 2023). Reconstructing drought episodes in this region and analyzing the response of white pine to these events may provide insights into the causes of their decline and support the development of future management strategies.

This study aims to *(i)* investigate the climatic signal in white pine tree-ring proxies (RW, $\delta^{13}C$, $\delta^{18}O$) under fast and moderate drainage conditions, and *(ii)* determine the combination of proxies offering the best potential for hydro-climate reconstructions. We expect the main climatic signal to be summer precipitation and temperatures because white pines are isohydric, but that this signal will be dependent on the drainage level. We also expect that combining multiple tree-ring proxies will lead to more reliable climate reconstructions than a single proxy.

2. Methods

2.1. Study area

Our study took place in the Opémican National Park, in the region of Témiscamingue, western Québec, Canada (46.84°N, 79.20°W; Fig. 1a). The Opémican National Park was created in 2018 and protects 25 300 ha of forests, including some of the oldest (~200 years) white pine stands in the Québec province (Sépaq, 2025). This area is located in the sugar maple (*Acer saccharum*) and yellow birch (*Betula alleghaniensis*) bioclimatic domain (MRNF, 2021). Surface deposits consist primarily of glacial and fluvio-glacial tills and moraines, but rocky outcrops are found at higher elevations (Gouvernement du Québec, 2024). The climate is subpolar continental, with cold winters and warm summers. Mean annual temperature is 5.1°C, with July (19.8°C) and January

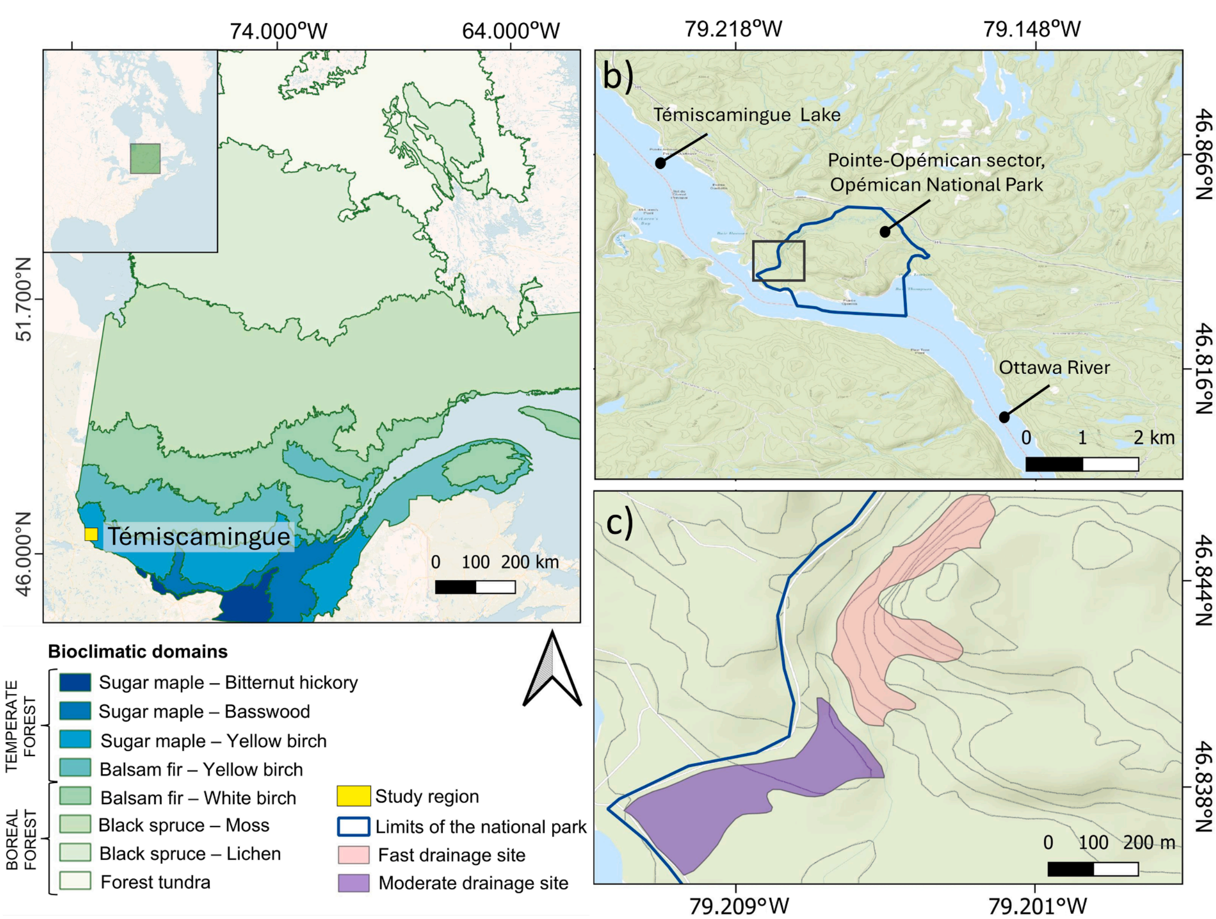

Fig. 1. (a) Location of the study region, (b) limits of the Pointe-Opémican sector of Opémican National Park, (c) the two sampling sites in Témiscamingue, western Québec, Canada.

(-10.8°C) being the warmest and coldest months, respectively. Yearly mean total precipitation is 892 mm, with monthly extremes in October (91 mm) and February (55.4 mm; Environnement Canada, 2024). The length of the growing season varies between 120 and 140 days (Natural resources Canada., 2016).

2.2. Field sampling

We conducted field sampling in the Pointe-Opémican sector of the Opémican National Park (Fig. 1b). We selected two sites based on their level of drainage and the presence of old-grown white pine stands: one site with fast drainage (average slope of 56°) located on the upper slope of a hill, and a site with moderate drainage (average slope of 6°) on the lower slope of the same hill (Fig. 1c, fig. S1). In the summer of 2023, we collected two 0.5-cm diameter cores at breast height on 30 dominant or co-dominant white pines in each site for ring width measurements (number of cores = 120; borer length = 60 cm). In the summer of 2024, we collected two 1.2-cm diameter cores on 10 trees per site for isotopic analysis (number of cores = 40; borer length = 40 cm). We chose dominant trees that looked the healthiest and without any apparent stem malformation or scars.

2.3. Dendrochronological approach

The 120 cores taken for ring width measurements were dried, glued on wooden supports and sanded with gradually smaller grain (80, 120, 220, 320, 400 grit). All samples were measured with CooRecorder (v. 9.8.0; Maxwell and Larsson, 2021) and were visually cross-dated before being cross-dated to calendar year with Past5 (v. 5.0.620; SCIEM 2021, Austria).

2.4. Isotopic measurements

2.4.1. Wood preparation

We flattened the 40 cores taken for isotopic measurements with a sliding manual microtome (core-microtome; Gärtner and Nievergelt, 2010) to avoid wood contamination between years. We then proceeded to the measurement with CooRecorder and cross-dating with Past5. For each site, we selected five 1.2-cm diameter cores from different trees according to the dating accuracy and the size of the growth rings (larger rings were preferred). We cut each ring of the 1950–2020 period with a razor blade and stored them individually, for a total of five samples per year per site (fig. S2). For each site, we pooled wood samples for every year by combining 6 mg of each sample, for a total of 71 samples containing 30 mg of wood per site. We homogenized the wood using 7-mm stainless steel balls in a MM 400 Mill Mixer (Retsch Milling & Sieving, France) for 3 min at 30 Hz. We transferred the homogenized wood samples to fibreglass filter bags (#F57 Ankom Technology, USA) for alpha-cellulose extraction.

2.4.2. Alpha-cellulose extraction

We followed the multi-step protocol presented in Namvar et al. (2024) to isolate alpha-cellulose. To remove soluble organic compounds from the wood samples, we placed the filter bags in a solution of toluene and ethanol (1:1) in an ultrasonic bath for 90 min, then boiled them in water for 60 min. To remove lignin, we placed the samples in water at 80°C and bleached them by adding sodium chlorite and acetic acid. To remove hemi-cellulose, we placed the samples in NaOH (17%) for 60 min, extensively rinsed them with distilled water, and immersed them with acetic acid (10%) for 10 min. We then rinsed the samples with distilled water until they reached a pH of 7 and let them dry for 24 h under the hood to obtain pure alpha-cellulose.

2.4.3. Mass spectrometry

The $\delta^{13}C$ and $\delta^{18}O$ measurements were conducted at the Geotop Light-Stable Isotope Geochemistry Laboratory (Université du Québec à Montréal, Montreal, Canada).

For $\delta^{13}C$ analysis, 0.5 mg of cellulose was weighed in tin capsules. The samples were analyzed using a Micromass Isoprime 100 isotope ratio mass spectrometer, connected to an Elementar Vario MicroCube elemental analyzer in continuous flow mode. The overall analytical uncertainty of the measurements was less than ±0.1‰ (Hélie and Hillaire-Marcel, 2021). For $\delta^{18}O$ analysis, 0.3 mg of cellulose was weighed in silver capsules. The samples were analyzed using an Isoprime VisIon isotope ratio mass spectrometer coupled to an Elementar Vario PyroCube elemental analyzer in continuous flow mode. The overall analytical uncertainty of the measurements was within ±0.3‰ (Hélie and Hillaire-Marcel, 2021).

2.5. Climatic data

We extracted monthly precipitation (mm/month) and mean temperature (°C) data for the 1950–2020 period from the ERA5 global reanalysis (Hersbach et al., 2023). We also extracted standardized precipitation evapotranspiration index values (SPEI; Vicente-Serrano et al., 2010) with accumulation windows of three months from the dataset of monthly drought indices derived from ERA5 reanalysis (European Centre for Medium-range Weather Forecast, 2025; Keune et al., 2025). SPEI is a normalized variable based on the balance between precipitation entering the system and potential evapotranspiration. Negative values indicate drier conditions compared to some reference period (here, 1991–2020), while positive values indicate wetter conditions. We used the same climatic data for both sampling sites because of the coarse spatial resolution of the data (0.25° x 0.25° in latitude and longitude).

2.6. Data processing

We averaged individual radial ring-width measurements for each tree, and detrended the resulting mean series per tree using a spline with a length corresponding to 67% of the series length with the dplR package in R (Bunn, 2008). We then created two mean chronologies, one per site, by averaging all individual detrended series in each site. We corrected the $\delta^{13}C$ data for the Suess effect (decreasing $\delta^{13}C$ of atmospheric CO_2) according to the equation of McCarroll et al. (2009). To do so, we used the reconstructed $\delta^{13}C$ atmospheric data from Belmecheri and Lavergne (2020) for the 1950–2014 period, and from Mathias and Hudiburg (2022) for the 2015–2020 period. We detected significant linear trends only in the mean temperature time series (fig. S3-S5), which could potentially bias interpretation at the interannual scale. To address this, we detrended the temperature data using a spline function, consistent with the method applied to ring-width measurements. We used the raw data for monthly precipitations, SPEI, and $\delta^{18}O$.

2.7. Statistical analyses

2.7.1. Proxy-climate relationship

To identify the climate variable most suitable for reconstructions, we tested the relationship between tree-ring proxies (ring width, $\delta^{13}C$, $\delta^{18}O$) and monthly climate data (mean temperature, total precipitation, and SPEI). We performed bootstrap correlation functions (1000 iterations) with the treeclim package in R (Zang and Biondi, 2015), testing temperature, precipitation and SPEI from the previous year (June to December) and the current year (January to September). Climate variables with the highest correlation coefficients amongst all tree-ring proxies, i.e. June and July total precipitation (pjj), June and July mean temperature (tjj), and June-August SPEI of the current year, were chosen as reconstruction targets. The stationarity of the response to climate was verified for the relevant proxies using a moving window analysis with 30-year windows and 5-year offsets.

2.7.2. Climate modeling

We used a linear model to model target climatic variables as a function of the three tree-ring proxies (ring width, $\delta^{13}C$, $\delta^{18}O$) and the drainage level. Drainage level was transformed into a binary vector of value 1 (fast drainage) or 0 (moderate drainage). The model used a Bayesian framework with Gibbs sampling implemented in JAGS (Plummer, 2003). We chose a Bayesian approach because it provides precise and reliable confidence intervals and enables us to assess the uncertainty of each parameter (Gennaretti et al., 2017). The model was written as follows:

$$target = \beta\_RWI * RWI + \beta\_\delta13C * \delta13C + \beta\_\delta18O * \delta18O + \beta\_drain * drainage + intercept \quad (1)$$

with ***target*** being either June and July precipitation (total), June and July temperature (mean) or June-August SPEI, ***β_RWI*** being the parameter associated with the effect of ring widths of the mean chronologies (RWI), ***β_δ13C*** being the parameter associated with the effect of $\delta^{13}C$, ***β_δ18O*** being the parameter associated with the effect of $\delta^{18}O$, ***β_drain*** being the parameter associated with the effect of drainage, and ***intercept*** being the intercept. The model assumes a normal distribution of observations (ERA5 values, **y**) around predicted values (***target***), with a standard deviation (***sd***) estimated by the model as follows:

$$y \sim N(\mu = target, \quad \sigma = sd) \quad (2)$$

We used non-informative priors for ***β_RWI, β_δ13C, β_δ18O, β_drain, intercept*** (normal distribution with a mean of 0 and a standard deviation of 100) and ***sd*** (uniform between 0 and 100). All parameters had initial values randomly selected from a normal distribution with a mean of zero and a standard deviation of one. Ten chains of 10,000 iterations, with a thinning rate of 10 and a burn-in of 1000, were executed with the JAGS program (v.4.3.2; Plummer, 2003) in R using the jagsUI package (Kellner, 2024). Full model code and diagnostic graphs are available in supplementary materials (fig. S6-S13).

Model reconstruction skill was evaluated by calculating the correlation between the predicted and observed climatic values. As the variance of the predicted climatic time series was lower than the observed one (Fig. S14), we re-scaled the predicted values by applying a correction to the standard deviation as follows:

$$pred_{corr} = \frac{pred - \overline{x}_{pred}}{s_{pred}} * s_{obs} + \overline{x}_{pred} \quad (3)$$

Where ***pred*** are the predicted values, $\overline{x}_{pred}$ is the mean of the predicted values, s_{pred} is the standard deviation of the predicted values, and s_{obs} is the standard deviation of the observed values. This rescaled time series was used for plotting the reconstruction.

All statistical analyses were performed in R (v. 4.3.3; R Core Team, 2021). Analyses were conducted for the 1950–2020 period (71 years) only, because it is the period covered by all the data.

3. Results

3.1. Tree-ring time series

For each of the three proxies, short- and long-term trends were similar between the two drainage levels, with correlation coefficients ranging from 0.76 to 0.81 (Fig. 2). The only proxy with significant

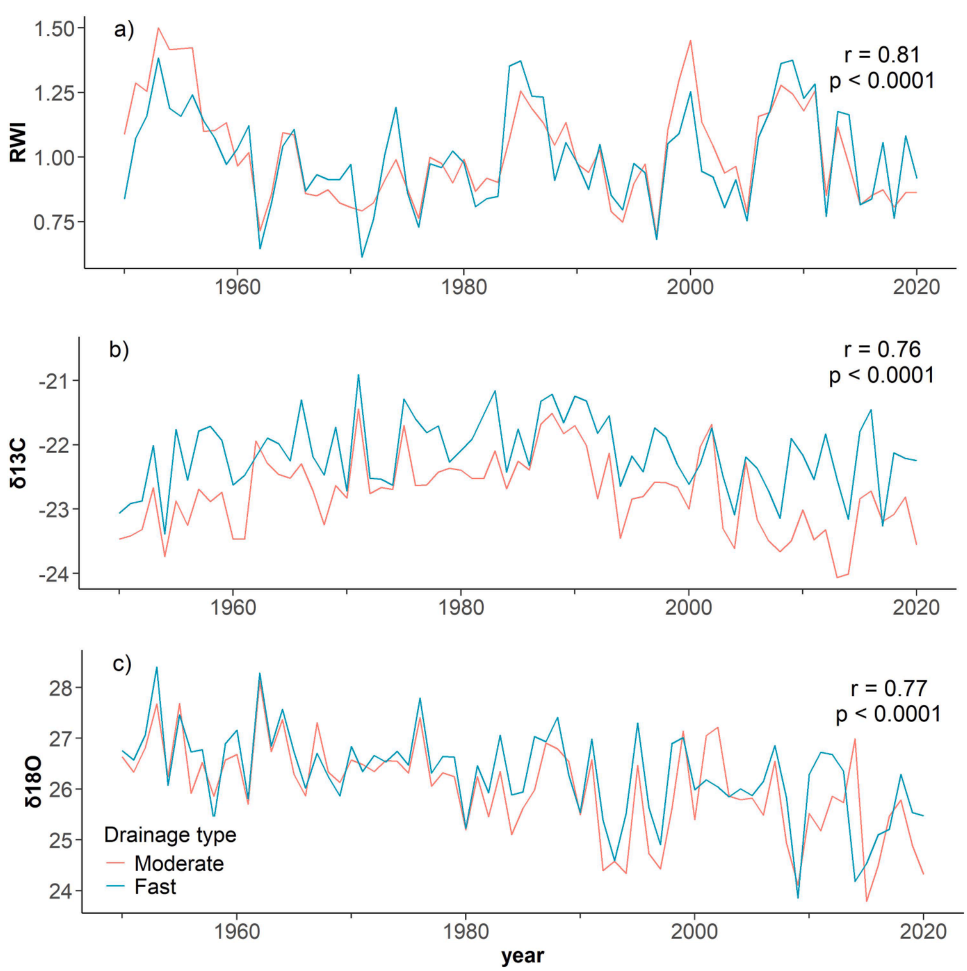

Fig. 2. (a) Chronologies of the detrended ring width (RWI), (b) carbon isotopic ratio ($\delta^{13}C$) and (c) oxygen isotopic ratio ($\delta^{18}O$) for the sites with fast (blue) and moderate (pink) drainage in the Opémican national park, Témiscamingue, western Québec. All chronologies cover the 1950–2020 period.

differences between sites was carbon isotopes, where $\delta^{13}C$ values were higher (+0.62, $p < 0.0001$) in the fast drainage site than in the moderate drainage site (fig. S15). Mean $\delta^{13}C$ time series were negatively correlated with mean ring width (RWI) time series (r = -0.34, p = 0.004) (fig. S16). No significant correlation was found between RWI and $\delta^{18}O$ (r = 0.09, p = 0.44) and $\delta^{13}C$ and $\delta^{18}O$ (r = 0.17, p = 0.16).

3.2. Proxy-climate relationship

At both sites, the strongest precipitation signal in tree-ring proxies was summer precipitation of the current year (Fig. 3). RWI was positively correlated with June and July precipitation at the fast drainage site, and June precipitation at the moderate drainage site (Fig. 3a-b). $\delta^{13}C$ was negatively correlated with June and July precipitation of the current year at both sites (Fig. 3c-d). $\delta^{18}O$ was not significantly correlated to summer precipitation but showed significant correlations with fall precipitation of the previous year at both sites, and the precipitation of April for the site with moderate drainage (Fig. 3e-f).

The strongest common temperature signal amongst the tree-ring proxies was the mean temperature of June and July of the current year (Fig. 4). $\delta^{13}C$ is positively correlated with June, July and August temperatures of the current year (Fig. 4c-d), while $\delta^{18}O$ is positively correlated with May, June and July temperatures of the current year (Fig. 4e-f). Although not always significant, RWI shows negative correlations with June and July temperatures of the current year (Fig. 4a-b).

The strongest common SPEI signal amongst the tree-ring proxies was summer SPEI of the current year (Fig. 5). RWI is positively correlated with June, July and August SPEI of the current year at the fast drainage site, while no significant correlation was found at the moderate drainage site (Fig. 5a-b). $\delta^{13}C$ is negatively correlated with June, July, August and September SPEI of the current year (Fig. 5c-d), while $\delta^{18}O$ is negatively correlated with June SPEI of the current year, and winter SPEI of the previous year (Fig. 5e-f).

Drainage level had limited effects on the proxies' response to climate variables. Indeed, only few differences were observed in correlation coefficients between the fast and moderate drainage sites (Figs. 3–5). The most significant difference was observed in the response of RWI to temperatures, where RWI of the moderate drainage site was positively correlated with the temperature of many more months than in the fast drainage site (Fig. 4a-b), and between RWI and SPEI, where no significant correlations were found at the moderate drainage site (Fig. 5b).

Moving window analysis revealed that RWI and $\delta^{13}C$ response to June and July precipitation, RWI and $\delta^{18}O$ response to June and July temperature, and RWI and $\delta^{13}C$ response to June-August SPEI was stationary over the 1950–2020 period (fig. S17-S19).

3.3. Climate modeling

Chain convergence was reached for all parameters (supplemental material; fig. S6-S8), and the posterior distributions of all parameters of the precipitation, temperature, and SPEI models were well defined and unimodal (Fig. 6). For the precipitation model, the 95% confidence intervals of all parameters excluded zero, except for the parameter

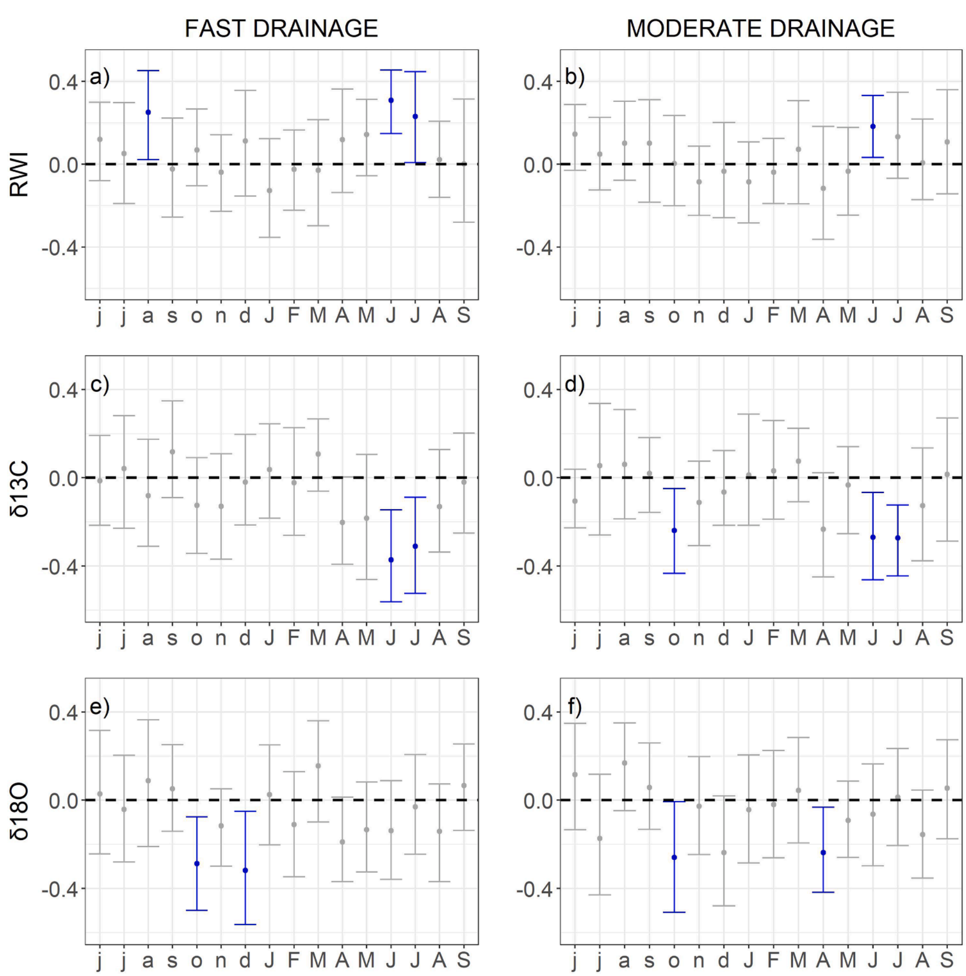

Fig. 3. Correlation coefficients between the tree-ring proxies (RWI, $\delta^{13}C$, $\delta^{18}O$) and monthly total precipitation in the fast (a, c, e) and moderate (b, d, f) drainage sites. Months of the previous year are in lowercase letters and months of the current year are in uppercase letters. Blue lines indicate significant correlations.

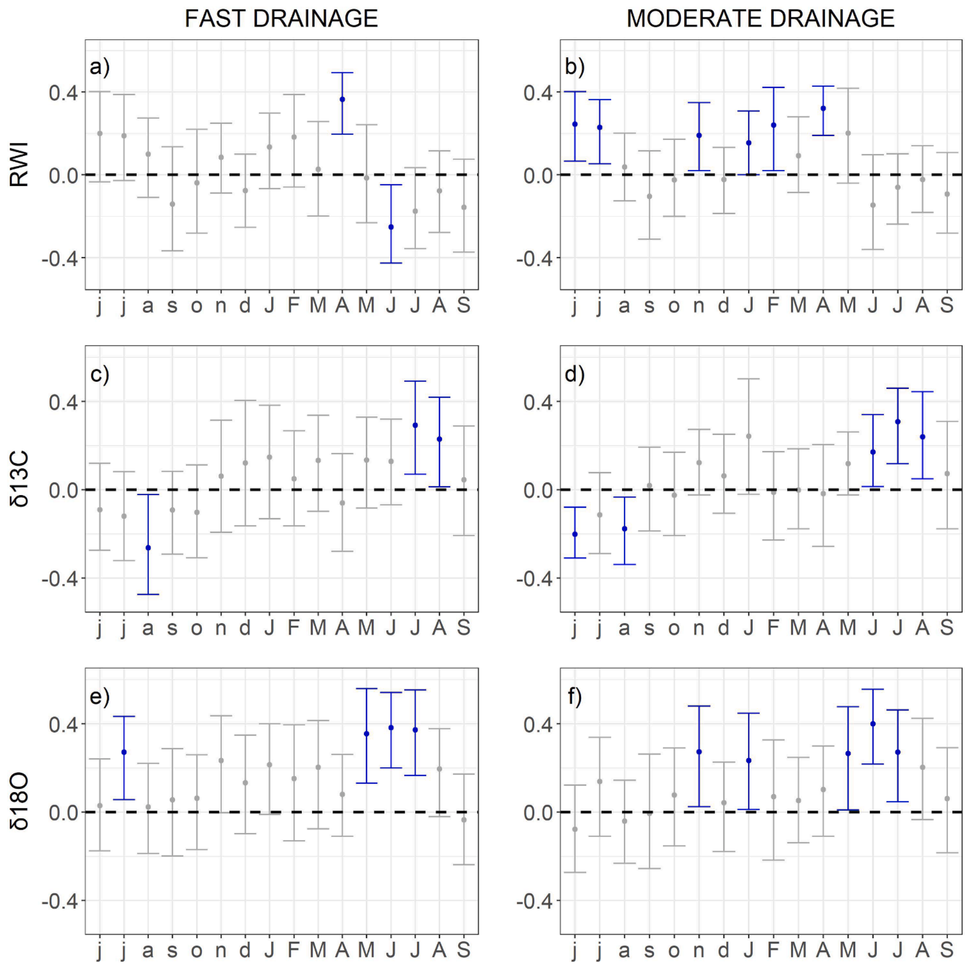

Fig. 4. Correlation coefficients between the tree-ring proxies (RWI, $\delta^{13}C$, $\delta^{18}O$) and monthly mean temperature in the fast (a, c, e) and moderate (b, d, f) drainage sites. Months of the previous year are in lowercase letters and months of the current year are in uppercase letters. Blue lines indicate significant correlations.

associated with $\delta^{18}O$ (Fig. 6, Table S1), indicating that RWI and $\delta^{13}C$ are the more useful proxies to reconstruct precipitation. For the temperature model, the confidence intervals of all parameters excluded zero, except for the parameters associated with $\delta^{13}C$ and drainage (Fig. 6, Table S1), indicating that RWI and $\delta^{18}O$ are the more useful proxies to reconstruct temperatures. For the SPEI model, the 95% confidence intervals of all parameters excluded zero, except for the parameter associated with RWI (Fig. 6, Table S1), indicating that $\delta^{13}C$ and $\delta^{18}O$ are the more useful proxies to reconstruct SPEI. These results also suggest that the drainage level has significant impact in the reconstruction of precipitations and SPEI, although the distribution was shifted toward negative values in the temperature model. The climatic data predicted by our models correlated closely with the climatic data extracted from the ERA5 database (Fig. 7). Indeed, Pearson correlation coefficients were 0.43, 0.49 and 0.45 for the predicted June and July precipitation, June and July temperature, and June-August SPEI, respectively.

4. Discussion

4.1. White pine's response to climate variations

The correlation analysis between the three tree-ring proxies and climate variables enabled us to better understand the physiological response of white pine to environmental variations. The main signal emerging from our data is the sensitivity of white pine to dry conditions.

We found a negative correlation between RWI and summer temperature and a positive correlation between RWI and summer precipitation and SPEI. These results imply that water stress is the main factor limiting radial growth of white pines in our study region. Our results are supported by previous studies that have found similar results (Chhin et al., 2018, 2013; Vose and Swank, 1994). Indeed, in western North Carolina, Vose and Swank (1994) observed a significant diminution of radial growth for white pines of all canopy classes during drought years. Moreover, while studying the radial growth response of white pines to climate in seven sites located at the northern edge of the distribution, Chhin et al. (2018) found that radial growth was negatively correlated with temperature and positively correlated with precipitation. However, sites with slower drainage are generally associated with higher water availability, thus making water availability less limiting (Chhin et al., 2013). This could explain why we did not find any significant correlations between SPEI and RWI at the moderate drainage site, and why RWI was positively correlated with temperature of some spring or summer months at the moderate drainage site. Nonetheless, the main climatic factors affecting radial growth were similar in both sites, as also observed by Chhin et al. (2013) when comparing the climatic signal of white pine radial growth in terrace versus floodway stands.

Increases in $\delta^{13}C$ are generally caused by increased photosynthetic activity or reduced stomatal conductance (McCarroll and Loader, 2004). White pines are isohydric, meaning that they exert tight stomatal regulation in response to water availability (Asbjornsen et al., 2021). The negative correlation between $\delta^{13}C$ and precipitation or SPEI found in this study suggests that the $\delta^{13}C$ signal was mainly associated with stomatal conductance. Moreover, the negative correlation between $\delta^{13}C$

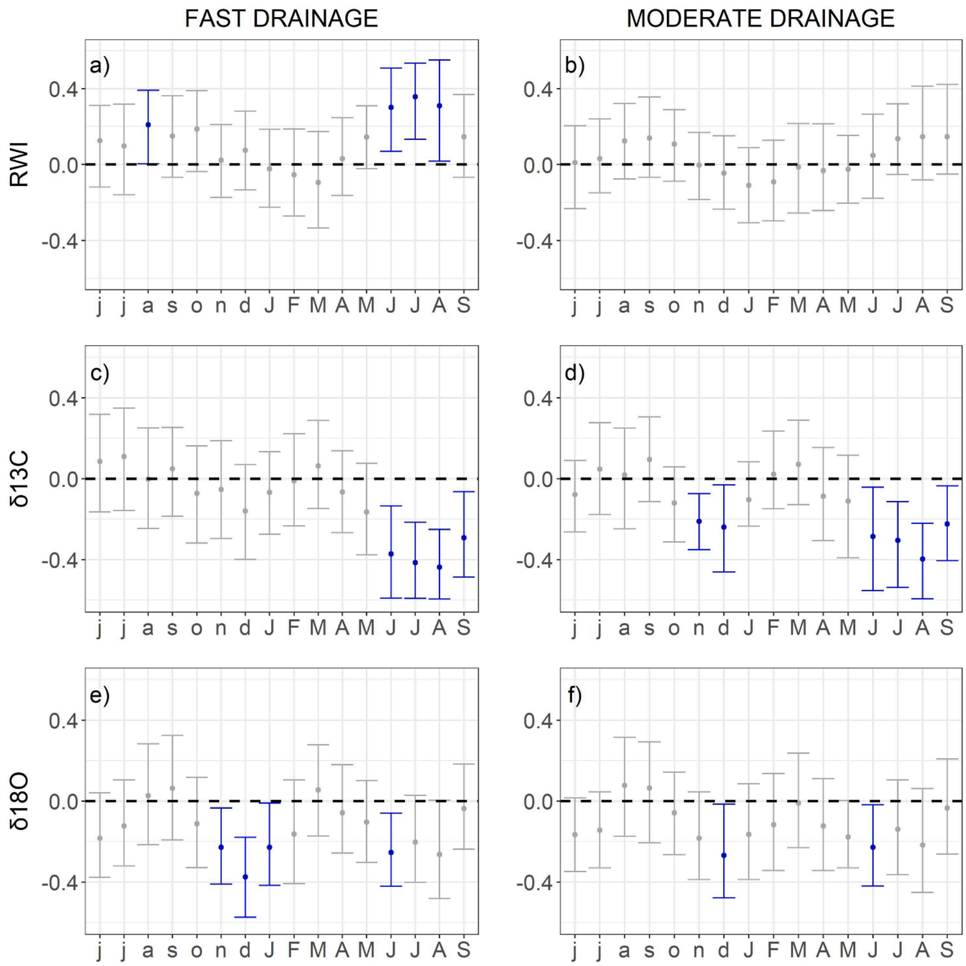

Fig. 5. Correlation coefficients between the tree-ring proxies (RWI, $\delta^{13}C$, $\delta^{18}O$) and SPEI (accumulation window of 3 months) in the fast (a, c, e) and moderate (b, d, f) drainage sites. Months of the previous year are in lowercase letters and months of the current year are in uppercase letters. Blue lines indicate significant correlations.

and RWI indicates that increases in $\delta^{13}C$ were not caused by an increase in photosynthetic rate, which should lead to an increase in wood formation and radial growth. Our results corroborate those from Asbjornsen et al. (2021) who also found a negative linear association between precipitation and $\delta^{13}C$ in white pine tree rings, and a major decrease in radial growth during induced drought episodes.

Our results revealed a positive correlation between $\delta^{18}O$ and summer (June and July) temperature, and a negative correlation with summer (June to August) SPEI, which also supports the theory of white pine's stomatal response to water stress. Indeed, warmer atmospheric temperature causes an increase in atmospheric vapor pressure deficit and higher evapotranspiration demand (Larcher, 2003). In this case, a subsequent enrichment in $\delta^{18}O$ demonstrates a reduced stomatal conductance, allowing for the preferential evapotranspiration of leaf water containing ^{16}O (Song et al., 2022). These results are supported by Maier and Teskey (1992) who observed a strong negative link between absolute humidity deficit and stomatal conductance in an experimental white pine forest in North Carolina, and by MacKay et al. (2012) who observed 27% less evapotranspiration in white pine stands subjected to induced drought. However, to our knowledge, our study is one of the first to demonstrate white pine's physiological response to water stress using $\delta^{18}O$. Another probable cause of increased $\delta^{18}O$ is the enrichment of soil water, caused by the accelerated evaporation of water from the soil in dry conditions (Siegwolf et al., 2023). This water, now enriched in $\delta^{18}O$, will subsequently be absorbed by the roots and used for photosynthesis (McCarroll and Loader, 2004). Unfortunately, we lack sufficient data to support this second explanation, and studies incorporating analyses of soil water isotopic composition could significantly strengthen this interpretation.

4.2. Climate reconstruction and the choice of proxies

The modeling of summer precipitation, temperature and SPEI enabled us to identify the most suitable tree-ring proxies for climate reconstruction using white pines. Our results also suggest that a multi-proxy approach is the most appropriate, with different proxy combinations allowing the reconstruction of different climate variables.

The posterior distribution of model parameters identified ring width and carbon isotopes as the best proxies for reconstructing June and July precipitation. When studying the potential for climate reconstruction using two pine species (Scots pine [*Pinus sylvestris*] and Mountain Pine [*Pinus uncinate*]), Gagen et al. (2006) also identified ring width and $\delta^{13}C$ as the best proxies for reconstructing summer precipitation. Our model also demonstrates that drainage level has an influence on the reconstruction of precipitation. The influence of drainage level can be explained by the constantly higher values of $\delta^{13}C$ in the fast drainage sites. These higher values are likely caused by the lower water availability due to the rapid drainage in this site, thus increasing white pine's leaf-level reaction to water stress. Consequently, there is a risk of over- or under-estimating the amount of precipitation if the type of drainage is unknown for sampled trees.

According to the model parameters, the best tree-ring proxies for

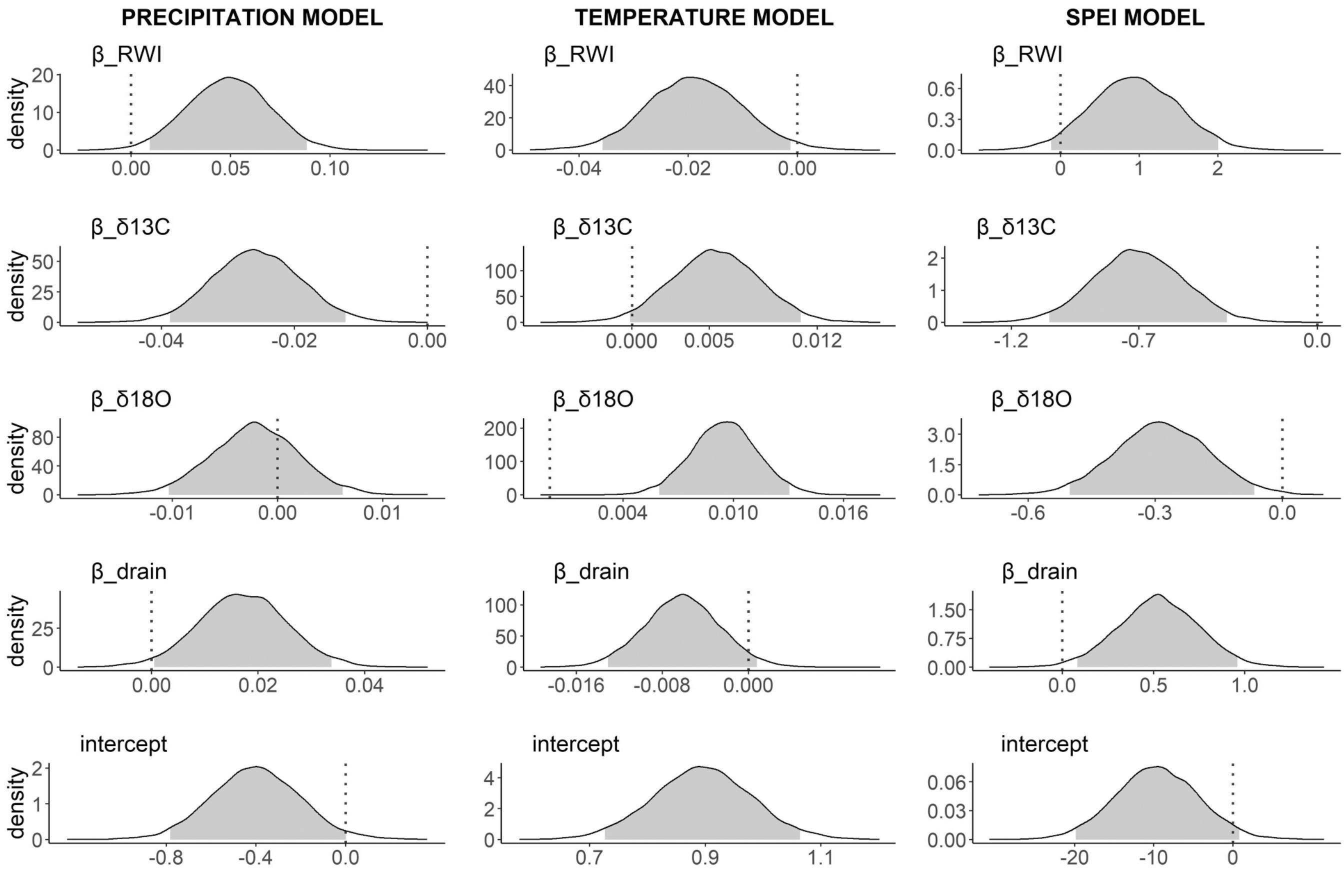

Fig. 6. Posterior distribution of the five parameters in the precipitation, temperature and SPEI Bayesian linear models. Shaded areas represent 95% confidence intervals, and vertical dotted lines highlight zero when present.

June and July temperature reconstruction are ring width and $\delta^{18}O$. Gennaretti et al. (2017) also identified ring width and $\delta^{18}O$ as the best two-proxy combination for reconstructing summer temperature with black spruce (*Picea mariana*) tree rings, although adding $\delta^{13}C$ also improved their model likelihood. In our temperature model, the drainage level was not identified as influencing the predicted temperature. The low effect of the drainage level in the temperature model could be attributed to the proximity of the two sites (at most 400 m apart) suggesting similar temperature at both locations. Therefore, the relative atmospheric humidity, evapotranspiration demand and the consecutive $\delta^{18}O$ enrichment would be equivalent in each site.

The posterior distribution of model parameters identified carbon and oxygen isotopes as the best proxies for reconstructing June-August SPEI. Because SPEI is a drought index that integrates precipitation and temperature, we expected the model to also identify RWI as a good proxy for reconstructing summer drought. In the initial correlation analysis, we found RWI to be related to SPEI only at the fast drainage site, probably because tree-growth is less limited by drought in sites where water is more accessible. This might be why the effect of RWI was not conclusive in the SPEI model. The expected difference in water accessibility between the fast and moderate drainage site might also explain why drainage level was identified as having an effect on SPEI reconstruction.

The three models suggested that the use of a multiproxy approach is favorable for climate reconstruction with white pine. Ring width, carbon isotopes and oxygen isotopes are influenced by different factors and therefore record different, and sometimes complementary, environmental signals (Hilasvuori et al., 2009). The combination of several proxies can produce more reliable climate reconstructions because it amplifies the common signal between proxies, while diminishing the uncertainties related to each single proxy (Sidorova et al., 2012). For example, when reconstructing summer temperatures in northern Québec using black spruce ring width, $\delta^{13}C$ and $\delta^{18}O$, Gennaretti et al. (2017) demonstrated that the posterior probability of their models was always narrower when multiple proxies were used. When reconstructing summer temperatures with Scots pine tree rings in Finland, Hilasvuori et al. (2009) found that the combination of ring width and carbon isotopes best accounted for proxies' discrepancies and amplify their common signal.

4.3. Potential of white pine for climate reconstruction

This study is among the first to evaluate the potential of white pine tree-ring parameters for reconstructing summer temperatures, precipitation and SPEI. To our knowledge, Voelker et al. (2019) is the only other study investigating the potential of using white pine tree rings for climate reconstruction in Canada, and they identified winter climate as a reconstruction target. They explained that the absence of summer climatic signal at their study site was caused by thermal inertia near Lake Superior, where the climate remains generally cold and humid throughout the summer (Voelker et al., 2019). In contrast to their study site, our study took place in a more xeric environment, where trees are subjected to a more variable summer climate.

The temperature, precipitation and SPEI reconstructed with our model correlated well with the observed data, indicating a good potential to reconstruct past climate variations. However, our reconstructions needed to be corrected for their variance, because the amplitude of the interannual variations was lower in the reconstructed than instrumental climate data (Fig. S14). This lower variance could be caused by the relatively low correlations between our climate proxies and the climate targets. Indeed, Robertson et al. (1999) demonstrated

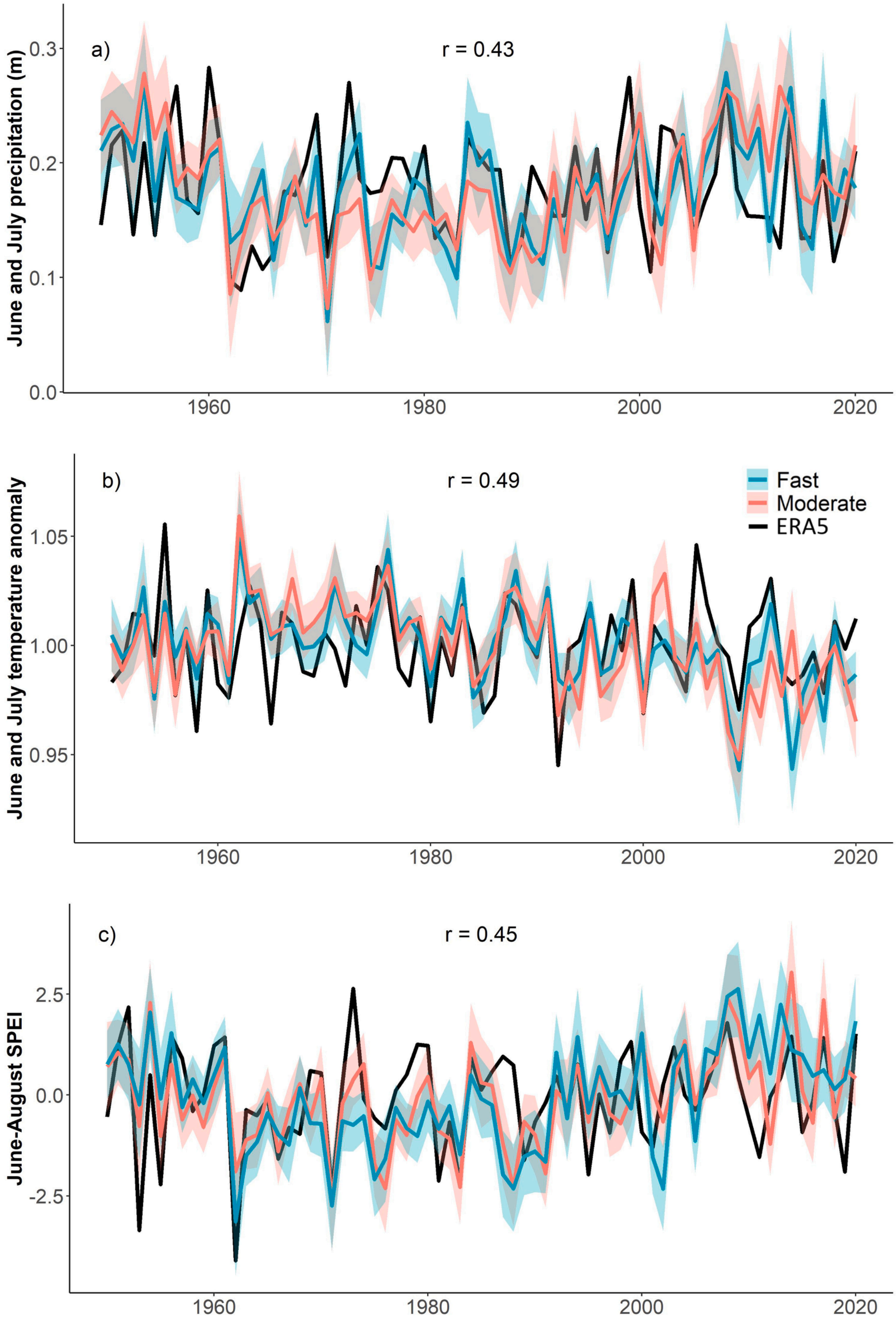

Fig. 7. June and July total precipitation (a), June and July mean temperature anomalies (b) and June-August SPEI (c)for the 1950–2020 period as obtained from the ERA5 dataset (black) or predicted by the linear Bayesian model (fast drainage; blue, moderate drainage; pink) with corrected standard deviation. Shaded areas represent 95% confidence intervals, and r values are the Pearson correlation coefficients between the observed and predicted data.

that there is almost always a systematic error in the variance of the reconstructed values, and that this error is inversely proportional to the initial single proxy-climate correlation. The main drawback of this error is that reconstructions underestimate the magnitude of extreme climatic events (Gagen et al., 2006). The simple mathematical correction that we applied to the predicted data enabled us to rescale the variance to the level of the climatic data from ERA5 and to correctly reconstruct the variability of the climate targets.

Although our models show a good potential for summer climate reconstruction with white pine tree rings, their application with sinker logs could be somewhat challenging because the drainage level was identified as influencing precipitation and drought reconstructions. Since the exact provenance of sinker logs is generally unknown, the drainage level to which they were subjected cannot be considered in the models. Therefore, we suggest that $\delta^{13}C$ of sinker logs be compared to that of live trees from different drainage levels prior to reconstruction to identify the drainage level and correct the predictions accordingly.

5. Conclusion

In this study, we demonstrated the potential of white pine tree rings to reconstruct past climate in temperate regions with yearly precision. We identified summer precipitation, temperature and SPEI as the main climatic factors affecting white pine growth, highlighting its sensitivity to water availability. Using Bayesian modeling, we determined that the best proxies for reconstructing summer temperature are ring width and oxygen isotopes, while the best proxies for summer precipitation are ring width and carbon isotopes and the best proxies for SPEI are carbon and oxygen isotopes. Because we found that the drainage level influences precipitation and drought reconstruction, the application of our models with sunken logs will require a priori determination of drainage level based on $\delta^{13}C$ data. To our knowledge, this study is the first to investigate a multi-proxy approach for summer climate reconstruction using white pine. These findings establish a robust basis for high-resolution reconstructions of summer climate across the distribution range of white pine. Moreover, advancing knowledge of white pine ecophysiology and its sensitivity to drought will improve our understanding of the probable causes of white pine decline and inform restoration efforts across its distribution range.

CRediT authorship contribution statement

Julie-Pascale Labrecque-Foy: Writing – review & editing, Writing – original draft, Visualization, Validation, Methodology, Investigation, Funding acquisition, Formal analysis, Data curation, Conceptualization. **Marc-André Lemay:** Writing – review & editing, Visualization, Software, Methodology, Formal analysis. **Fabio Gennaretti:** Writing – review & editing, Validation, Supervision, Software, Resources, Methodology, Formal analysis. **Étienne Boucher:** Writing – review & editing, Resources, Methodology, Conceptualization. **Dominique Arseneault:** Writing – review & editing, Supervision, Methodology. **Miguel Montoro Girona:** Writing – review & editing, Validation, Supervision, Software, Resources, Project administration, Methodology, Investigation, Funding acquisition, Conceptualization.

Funding

This research was funded by the Natural Sciences and Engineering Research Council of Canada (NSERC) discovery grant to reconstruct the regime of natural disturbances in forest ecosystems (RGPIN-2022–05423). First author was supported by the excellence scholarship programs from Vanier Canada Graduate Scholarships (CGV-180844) and the Fonds de Recherche du Québec – Nature et Technologies (315933).

Declaration of Competing Interest

The authors declare that they have no known competing financial interests or personal relationships that could have appeared to influence the work reported in this paper.

Acknowledgements

The authors would like to thank the Opémican National Park team for their help and collaboration with fieldwork. They would also like to thank the field assistants, E Berthiaume et E Gilles, and colleague M. Alcalá Pajares for their precious help. Lastly, the authors would like to thank the GEOTOP team, A Adamowicz-Walczak, J-F Hélie and S Namvar, for their help with lab work and isotopic analysis.

Appendix A. Supporting information

Supplementary data associated with this article can be found in the online version at doi:10.1016/j.dendro.2026.126507.

Data availability

Data will be made available on request.

References

Aird, P.L., 2016. Logging and rafting square timber in Ontario and Québec for shipment to Great Britain circa 1870–1908. For. Chron. 92, 394–400. https://doi.org/10.5558/tfc2016-072.

Asbjornsen, H., McIntire, C.D., Vadeboncoeur, M.A., Jennings, K.A., Coble, A.P., Berry, Z. C., 2021. Sensitivity and threshold dynamics of *Pinus strobus* and *Quercus* spp. in response to experimental and naturally occurring severe droughts. Tree Physiol. 41, 1819–1835. https://doi.org/10.1093/treephys/tpab056.

Belmecheri, S., Lavergne, A., 2020. Compiled records of atmospheric CO2 concentrations and stable carbon isotopes to reconstruct climate and derive plant ecophysiological indices from tree rings. Dendrochronologia 63, 125748. https://doi.org/10.1016/j.dendro.2020.125748.

Bunn, A.G., 2008. A dendrochronology program library in R (dplR). Dendrochronologia 26, 115–124. https://doi.org/10.1016/j.dendro.2008.01.002.

Büntgen, U., Esper, J., 2025. The need for high-resolution paleoclimate research. Dialog. Clim. Change 2, 18–25. https://doi.org/10.1177/29768659241305959.

Chhin, S., Chumack, K., Dahl, T., David, E.T., Kurzeja, P., Magruder, M., Telewski, F.W., 2013. Growth-climate relationships of *Pinus strobus* in the floodway versus terrace forest along the banks of the Red Cedar River, Michigan. TreeRing Res. 69, 37–47. https://doi.org/10.3959/1536-1098-69.2.37.

Chhin, S., Zalesny, R.S., Parker, W.C., Brissette, J., 2018. Dendroclimatic analysis of white pine (Pinus strobus L.) using long-term provenance test sites across eastern North America. For. Ecosyst. 5 (1), 18. https://doi.org/10.1186/s40663-018-0136-0.

Danneyrolles, V., Arseneault, D., Bergeron, Y., 2016. Long-term compositional changes following partial disturbance revealed by the resurvey of logging concession limits in the northern temperate forest of eastern Canada. Can. J. For. Res. 46, 943–949. https://doi.org/10.1139/cjfr-2016-0047.

Duffy, J.E., McCarroll, D., Loader, N.J., Young, G.H.F., Davies, D., Miles, D., Bronk Ramsey, C., 2019. Absence of age-related trends in stable oxygen isotope ratios from Oak Tree Rings. Glob. Biogeochem. Cycles 33, 841–848. https://doi.org/10.1029/2019GB006195.

Environnement Canada, 2024. Données historiques - Barrage Témiscamingue [WWW Document]. URL ⟨https://climat.meteo.gc.ca/historical_data/search_historic_data_f.html⟩ (accessed 8.27.24).

European Centre for Medium-range Weather Forecast, 2025. Monthly drought indices from 1940 to present derived from ERA5 reanalysis [WWW Document]. ECMWF Cross Data Store (ECDS). https://doi.org/10.24381/9bea5e16.

Gagen, M., McCarroll, D., Edouard, J.-L., 2006. Combining ring width, density and stable carbon isotope proxies to enhance the climate signal in tree-rings: an example from the southern French Alps. Clim. Change 78, 363–379. https://doi.org/10.1007/s10584-006-9097-3.

Gärtner, H., Nievergelt, D., 2010. The core-microtome: A new tool for surface preparation on cores and time series analysis of varying cell parameters. Dendrochronologia 28, 85–92. https://doi.org/10.1016/j.dendro.2009.09.002.

Gennaretti, F., Arseneault, D., Nicault, A., Perreault, L., Bégin, S., 2014. Volcano-induced regime shifts in millennial tree-ring chronologies from northeastern North America. Proc. Natl. Acad. Sci. 111, 10077–10082. https://doi.org/10.1073/pnas.1324220111.

Gennaretti, F., Huard, D., Naulier, M., Savard, M., Bégin, C., Arseneault, D., Guiot, J., 2017. Bayesian multiproxy temperature reconstruction with black spruce ring widths and stable isotopes from the northern Quebec taiga. Clim. Dyn. 49, 4107–4119. https://doi.org/10.1007/s00382-017-3565-5.

Gouvernement du Québec, 2024. Forêt Ouverte [WWW Document]. URL ⟨https://www.foretouverte.gouv.qc.ca/⟩ (accessed 8.27.24).

Grudd, H., 2008. Torneträsk tree-ring width and density ad 500–2004: a test of climatic sensitivity and a new 1500-year reconstruction of north Fennoscandian summers. Clim. Dyn. 31, 843–857. https://doi.org/10.1007/s00382-007-0358-2.

Hélie, J.F., Hillaire-Marcel, C., 2021. Designing working standards for stable H, C, and O isotope measurements in CO2 and H2O. Rapid Commun. Mass Spectrom. 35, e9008. https://doi.org/10.1002/rcm.9008.

Hersbach, H., Bell, B., Berrisford, P., Biavati, G., Horányi, A., Muñoz Sabater, J., Nicolas, J., Peubey, C., Radu, R., Rozum, I., Schepers, D., Simmons, A., Soci, C., Dee, D., Thépaut, J.-N., 2023. ERA5 monthly averaged data on single levels from 1940 to present [dataset]. https://doi.org/10.24381/cds.f17050d7.

Hilasvuori, E., Berninger, F., Sonninen, E., Tuomenvirta, H., Jungner, H., 2009. Stability of climate signal in carbon and oxygen isotope records and ring width from Scots pine (Pinus sylvestris L.) in Finland. J. Quat. Sci. 24, 469–480. https://doi.org/10.1002/jqs.1260.

Kellner, K., 2024. jagsUI: A Wrapper Around "rjags" to Streamline "JAGS" Analyses. R. Package Version 1 (6), 2.

Keune, J., Di Giuseppe, F., Barnard, C., Damasio da Costa, E., Wetterhall, F., 2025. ERA5–drought: global drought indices based on ECMWF reanalysis. Sci. Data 12, 616. https://doi.org/10.1038/s41597-025-04896-y.

Labrecque-Foy, J.-P., Montoro Girona, M., 2023. The global potential of log-driven trees for reconstructing forest ecosystems dynamics. Front. Ecol. Evol. 11, 1232543. https://doi.org/10.3389/fevo.2023.1232543.

Larcher, W., 2003. Physiological plant ecology: ecophysiology and strees physiology of functional groups. Springer Verlang, Berlin, Germany, p. 513.

Liu, Y., Zhang, X., Song, H., Cai, Q., Li, Q., Zhao, B., Liu, H., Mei, R., 2017. Tree-ring-width-based PDSI reconstruction for central Inner Mongolia, China over the past 333 years. Clim. Dyn. 48, 867–879. https://doi.org/10.1007/s00382-016-3115-6.

MacKay, S.L., Arain, M.A., Khomik, M., Brodeur, J.J., Schumacher, J., Hartmann, H., Peichl, M., 2012. The impact of induced drought on transpiration and growth in a temperate pine plantation forest. Hydrol. Process. 26, 1779–1791. https://doi.org/10.1002/hyp.9315.

Maier, C.A., Teskey, R.O., 1992. Internal and external control of net photosynthesis and stomatal conductance of mature eastern white pine (*Pinus strobus*. Can. J. For. Res. 22, 1387–1394. https://doi.org/10.1139/x92-184.

Mathias, J.M., Hudiburg, T.W., 2022. isocalcR: An R package to streamline and standardize stable isotope calculations in ecological research. Glob. Change Biol. 28, 7428–7436. https://doi.org/10.1111/gcb.16407.

Maxwell, R.S., Larsson, L.-A., 2021. Measuring tree-ring widths using the CooRecorder software application. Dendrochronologia 67, 125841. https://doi.org/10.1016/j.dendro.2021.125841.

McCarroll, D., Gagen, M.H., Loader, N.J., Robertson, I., Anchukaitis, K.J., Los, S., Young, G.H.F., Jalkanen, R., Kirchhefer, A., Waterhouse, J.S., 2009. Correction of tree ring stable carbon isotope chronologies for changes in the carbon dioxide content of the atmosphere. Geochim. Et. Cosmochim. Acta 73, 1539–1547. https://doi.org/10.1016/j.gca.2008.11.041.

McCarroll, D., Loader, N.J., 2004. Stable isotopes in tree rings. Quat. Sci. Rev. 23, 771–801. https://doi.org/10.1016/j.quascirev.2003.06.017.

MRNF, 2021. Classification écologique du territoire québécois. Direction des inventaires forestiers. gouvernement du Québec, p. 11.

Namvar, S., Boucher, É., Deslauriers, A., Morin, H., Savard, M.M., 2024. Monitoring weekly δ13C variations along the cambium–xylem continuum in the Canadian eastern boreal forest. Tree Physiol. 44, tpae136. https://doi.org/10.1093/treephys/tpae136.

Natural resources Canada, 2016. Gorwing season length 1981-2010 [WWW Document]. URL ⟨https://cfs.nrcan.gc.ca/fc-data-catalogue/read/23⟩ (accessed 5.8.25).

Naulier, M., Savard, M.M., Bégin, C., Gennaretti, F., Arseneault, D., Marion, J., Nicault, A., Bégin, Y., 2015. A millennial summer temperature reconstruction for northeastern Canada using oxygen isotopes in subfossil trees. Climate 11, 1153–1164. https://doi.org/10.5194/cp-11-1153-2015.

Plummer, M., 2003. JAGS: A Program for Analysis of Bayesian Graphical Models using Gibbs Sampling. Presented at the Proceedings of the 3rd International Workshop on Distributed Statistical Computing, Proceedings of the 3rd International Workshop on Distributed Statistical Computing. Vienna, Austria, p. 10.

R Core Team, 2021. R: A language and environment for statistical computing, R Foundation for Statistical Computing, Vienna, Austria. URL ⟨https://www.R-project.org/⟩. ed.

Rinne, K.T., Loader, N.J., Switsur, V.R., Waterhouse, J.S., 2013. 400-year May–August precipitation reconstruction for Southern England using oxygen isotopes in tree rings. Quat. Sci. Rev. 60, 13–25. https://doi.org/10.1016/j.quascirev.2012.10.048.

Robertson, I., Lucy, D., Baxter, L., Pollard, A.M., Aykroyd, R.G., Barker, A.C., Carter, A.H. C., Switsur, V.R., Waterhouse, J.S., 1999. A kernel-based Bayesian approach to climatic reconstruction. Holocene 9, 495–500. https://doi.org/10.1191/095968399676373488.

Robles, D., Boulanger, Y., Pascual, J., Danneyrolles, V., Bergeron, Y., Drobyshev, I., 2025. Timber harvesting was the most important factor driving changes in vegetation composition, as compared to climate and fire regime shifts, in the mixedwood temperate forests of Temiscamingue since AD 1830. Land. Ecol. 40, 26. https://doi.org/10.1007/s10980-025-02043-x.

Sarris, D., Siegwolf, R., Körner, C., 2013. Inter- and intra-annual stable carbon and oxygen isotope signals in response to drought in Mediterranean pines. Agric. For. Meteorol. 168, 59–68. https://doi.org/10.1016/j.agrformet.2012.08.007.

Sedell, J.R., Leone, F.N., Duval, W.S., 1991. Chapter 9: Water transportation and ttorage of logs, in: Influences of Forest and Rangeland Management on Salmonid Fishes and Their Habitats. Am. Fish. Soc. Spec. Publ. 325–368.

Sépaq, 2025. Opémican National Park [WWW Document]. URL ⟨https://www.sepaq.com/pq/ope/index.dot?language_id=1⟩ (accessed 5.8.25).

Shestakova, T.A., Martínez-Sancho, E., 2021. Stories hidden in tree rings: a review on the application of stable carbon isotopes to dendrosciences. Dendrochronologia 65, 125789. https://doi.org/10.1016/j.dendro.2020.125789.

Sidorova, O.V., Saurer, M., Myglan, V.S., Eichler, A., Schwikowski, M., Kirdyanov, A.V., Bryukhanova, M.V., Gerasimova, O.V., Kalugin, I.A., Daryin, A.V., Siegwolf, R.T.W., 2012. A multi-proxy approach for revealing recent climatic changes in the Russian Altai. Clim. Dyn. 38, 175–188. https://doi.org/10.1007/s00382-010-0989-6.

Siegwolf, R.T.W., Lehmann, M.M., Goldsmith, G.R., Churakova (Sidorova), O.V., Mirande-Ney, C., Timoveeva, G., Weigt, R.B., Saurer, M., 2023. Updating the dual C and O isotope—Gas-exchange model: A concept to understand plant responses to the environment and its implications for tree rings. Plant. Cell & Environ. 46, 2606–2627. https://doi.org/10.1111/pce.14630.

Song, X., Lorrey, A., Barbour, M.M., 2022. Chapter 10: EnvironMental, Physiological and Biochemical Processes Determining the Oxygen Isotope Ration of Tree-ring Cellulose. Stable Isot. Tree Rings Inferring Physiol. Clim. Environ. Responses 311–329.

Uprety, Y., Asselin, H., Bergeron, Y., 2013. Cultural importance of white pine (*Pinus strobus* L.) to the Kitcisakik Algonquin community of western Quebec, Canada. Can. J. For. Res. 43, 544–551. https://doi.org/10.1139/cjfr-2012-0514.

Vicente-Serrano, S.M., Beguería, S., López-Moreno, J.I., 2010. A multiscalar drought index sensitive to global warming: the standardized precipitation evapotranspiration index. J. Clim. 23, 1696–1718. https://doi.org/10.1175/2009JCLI2909.1.

Voelker, S.L., Wang, S.-Y.S., Dawson, T.E., Roden, J.S., Still, C.J., Longstaffe, F.J., Ayalon, A., 2019. Tree-ring isotopes adjacent to Lake Superior reveal cold winter anomalies for the Great Lakes region of North America. Sci. Rep. 9, 4412. https://doi.org/10.1038/s41598-019-40907-w.

Vose, J.M., Swank, W.T., 1994. Effects of long-term drought on the hydrology and growth of a white pine plantation in the southern Appalachians. For. Ecol. Manag. 64, 25–39. https://doi.org/10.1016/0378-1127(94)90124-4.

Zang, C., Biondi, F., 2015. treeclim: an R package for the numerical calibration of proxy-climate relationships. Ecography 38, 431–436. https://doi.org/10.1111/ecog.01335.